Dalton Transactions

An international journal of inorganic chemistry

Accepted Manuscript

Volume 46
Number 10
14 March 2017
Pages 3073-3412

Dalton Transactions

An international journal of inorganic chemistry

rsc.li/dalton

ISSN 0306-0012

ROYAL SOCIETY OF CHEMISTRY

COMMUNICATION
Douglas W. Stephen et al
N-Heterocyclic carbene stabilized parent sulfenyl, selenenyl, and tellurenyl cations (XH⁺; X = S, Se, Te)

ROYAL SOCIETY OF CHEMISTRY

ARTICLE

Post-synthetic Anion Exchange in Iron(II) 1,2,4-Triazole Based Spin Crossover Materials via Mechanochemistry

Jed H. Askew,[a] and Helena J. Shepherd[*a]

A facile method for post-synthetic exchange of anions in an iron(II) spin crossover material using mechanochemistry is described. Dry grinding of the $[Fe(atrz)_3]Cl_2$ complex (atrz = 4-amino-1,2,4-triazole) in the presence of an excess of sodium halide salt results in the complete exchange of anions and formation of $[Fe(atrz)_3]Br_2$ and $[Fe(atrz)_3]I_2$ in a solid-state metathesis reaction. The method represents a new strategy for tuning active switching properties such as the transition temperature in spin crossover systems. Formation of stable by-products was identified as a major driving force for exchange and a straightforward method to predict the likely outcome of such reactions using simple thermodynamic considerations is presented.

Introduction

Spin crossover (SCO) materials undergo reversible switching between low spin (LS) and high spin (HS) states in response to external stimuli such as temperature,[1] pressure,[2] light irradiation[3] and guest molecules.[4] The switching causes a change in their colour, structure and magnetic properties and is often accompanied by thermal hysteresis, conferring bistability onto these systems. Advances in recent years have led to a surge of interest in SCO materials for sensing,[5] display[6] and actuator technologies.[7]

One-dimensional coordination polymers formed from complexation of Fe^{2+} with 4-substituted-1,2,4-triazole (Rtrz) ligands, with general formula $[Fe(Rtrz)_3](A)_2 \cdot xH_2O$ (where A = BF_4, Cl, ClO_4 and x = 0 − 3, Scheme 1(a)) are an area of particularly intensive research within the field of SCO materials. These materials have shown great potential for application due to the high degree of cooperativity of the SCO event and the high temperature of operation that many of these materials exhibit, even at the nanoscale. Synthesis of nanoparticles of iron triazole complexes yields materials that display abrupt SCO and thermal bistability even at very small length scales, which increases their versatility for integration with a range of technologies.[8] These coordination polymers are generally stable in air and offer substantial possibilities for chemical modification, which can be used to tune the switching properties towards specific technological requirements. The SCO properties are strongly dependant on the R-group in the 4-position, the anion and the degree of hydration.[9,10] Recent reports have successfully shown the potential to tune the SCO behaviour of these coordination polymers through post-synthetic modification of the substituent in that position.[11,12]

The $[Fe(atrz)_3]A_x$ subset of complexes (where atrz = 4-amino-4H-1,2,4-triazole, A = anion) has been thoroughly explored with more than 30 different anions used to synthesise SCO-active materials.[10] In the first instance, synthesis of these materials appears straightforward, with the reaction of the appropriate iron(II) salt and triazole in a 1:3 ratio in hot aqueous or alcoholic solution leading to rapid precipitation of the active material.[13] However, such simple synthesis is limited by commercial availability of the corresponding iron salt, usually $Fe(BF_4)_2$, $FeCl_2$, or $Fe(ClO_4)_2$.[9] Other anions that have be used in this family often require the *in-situ* formation of the $[Fe(H_2O)_6]A_x$ complex from iron powder and the corresponding acid.[14] This process can significantly increase reaction times and the corrosive nature of the acids increases synthetic complexity,[9] reducing the likelihood of adoption of materials with more exotic anions for industrial-scale applications.

Recently, we reported the solvent-free synthesis of a range of SCO materials (including iron triazole complexes) *via* mechanochemistry. The facile procedure yields products that maintain SCO behaviour, with cooperativity comparable to standard solution-state techniques.[15] Mechanochemistry refers to the application of mechanical energy to drive a chemical reaction, and is a technique increasingly used in many other fields, including organic synthesis,[16–19] coordination chemistry,[20,21] co-crystal formation[22] and supramolecular networks.[20,23,24]

a. *Supramolecular, Interfacial & Synthetic Chemistry Group, School of Physical Sciences, University of Kent, Canterbury, CT2 7NH, UK*
b. *E-mail: h.j.shepherd@kent.ac.uk*

ARTICLE
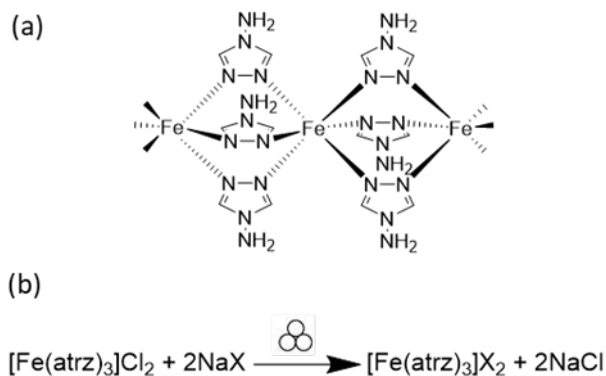
Scheme 1: (a) Schematic representation of 1-D triazole chains with 4-amino-1,2,4-triazole. (b) Reaction schematic for SSM of [Fe(atrz)$_3$]Cl$_2$, where X = Br, I

Mechanical energy can also be applied to a material *after* synthesis to further chemically modify it, for example through solid state metathesis (SSM). SSM is a technique commonly used in the synthesis of inorganic materials as a 'double displacement' reaction initiated by external stimuli such as ignition sources, microwave or mechanical energy.[25–27] SSM reactions use the intrinsically available energy of reacting species to promote the exchange of ions between compounds. Applications of SSM are thus far mostly limited to the synthesis of solid-state materials such as metal borides, nitrides and carbides, with particular interest in the synthesis of novel rare earth salts such as nitridoborates and carbodiimides, in yields and speeds inaccessible via direct synthetic routes.[28] In most SSM reactions, the formation of highly stable alkali halide salts acts as the primary driving force for the reaction.[25] The majority of successful SSM reactions are the result of very large enthalpies of reaction ($\Delta H_{rxn}°$) and, as such, the reactions are usually rapid and self-sustaining.[29]

Previous studies on post-synthetic grinding of solution-synthesised SCO materials have been conducted by monitoring the change in SCO properties of a material as a function of grinding duration.[30-32] It was found that the number of defects in the lattice increased with time as a result of mechanical strain induced by the high-energy ball mills used in these studies.[32] The effect on the SCO properties is an increase in residual HS fraction at low temperature, a decrease in the abruptness of the transition, a slight decrease in the transition temperature and a significant decrease in hysteresis. Size-reduction can lead to very similar changes in SCO properties,[33] and differentiating between the effects of size reduction and introduction of defects is not trivial.[32,33]

Herein we present the application of SSM to the post-synthetic modification of the SCO system [Fe(atrz)$_3$]Cl$_2$ to exchange the chloride anions for bromide and iodide according to Scheme 1(b).

Experimental

All reagents were purchased from Fisher Scientific and were used as received without additional purification. All mechanochemical experiments were conducted in air under ambient conditions using a glass pestle and mortar.

Compound **1**: [Fe(atrz)$_3$]Cl$_2$ was prepared by grinding iron(II) chloride tetrahydrate (4.00 g, 20.12 mM) and 4-amino-4*H*-1,2,4-triazole (5.10 g, 60.66 mM) in a glass pestle and mortar in the absence of solvent. Within 2 minutes of grinding, the sample became a wet purple paste. Continuous grinding for a total of 10 minutes resulted in a dry purple powder. The resulting powder was washed using a 9:1 mixture of methanol and water containing L-ascorbic acid (2% by mass), filtered and dried under vacuum at 45°C, yielding a fine purple powder (7.20 g, 94.5% yield).

Solid state metathesis reaction procedure: Compound **1** (0.5 g, 1.32 mM) and the corresponding sodium salt (in a five-fold excess) were ground in a glass pestle and mortar in the absence of solvent for 15 minutes. The resulting powder was collected and washed using a 9:1 mixture of methanol and water containing L-ascorbic acid (2% by mass), filtered, and dried under vacuum at 45°C. Washing of all products was carried out using this method to maintain consistency, irrespective of the relative solubilities of the sodium salts used.

CAUTION: Do not use mechanochemical techniques for the preparation or modification of potentially explosive materials. Perchlorate salts and tetrazole ligands are occasionally used in SCO research. Both of these have the potential to explode when handled dry, particularly on contact or grinding, and thus should not be used in routine mechanochemical experiments.

Magnetic susceptibility measurements were performed using a Quantum Design MPMS SQUID magnetometer. Temperature dependent measurements were made using a 1000 Oe magnetic field across the stated temperature ranges, while ramping the temperature at a rate of 2 K min^{-1}. PXRD data were collected at room temperature using a Rigaku MiniFlex 600 desktop X-ray diffractometer using Cu Kα radiation. TEM was performed using a Jeol 1230 120 kV transmission electron microscope equipped with a Gatan One View 16mp camera with automatic drift correction.

Scherrer analysis of compound **1** and compound **1-Cl**, was carried out using powder X-ray diffraction data collected on a Panalytical X'Pert3 using Cu Kα radiation. EDX measurements were recorded using a Hitachi-3400n SEM fitted with an Oxford Instruments X-Max 80mm^2 SDD. Full details of analytical techniques are provided in the supporting information.

$T_{1/2}\uparrow$ and $T_{1/2}\downarrow$ are defined as the midpoint for the transition in the second heating and cooling cycles respectively. 'Smoothness' is defined as the difference in the temperature for which 80% and 20% of the complexes are in the HS state, as previously described.[35]
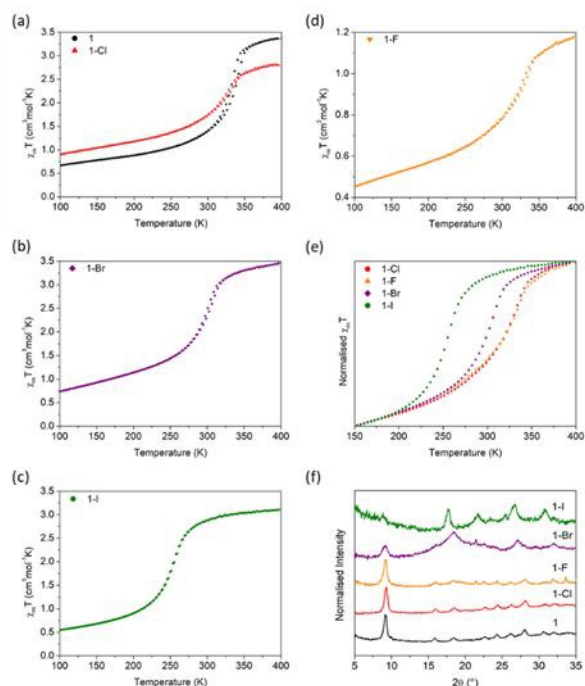
ARTICLE

Figure 1: Comparison of $X_M T$ vs T for **1** and **1-Cl** (a), **1-Br** (b), **1-I** (c), **1-F** (d). Normalised second Heating cycle for **1**, **1-Cl**, **1-Br** and **1-F** between 150 to 400 K (e). Comparison of normalised PXRD data bottom to top: **1** (black), **1-Cl** (red), **1-F** (orange), **1-Br** (purple) and **1-I** (green).
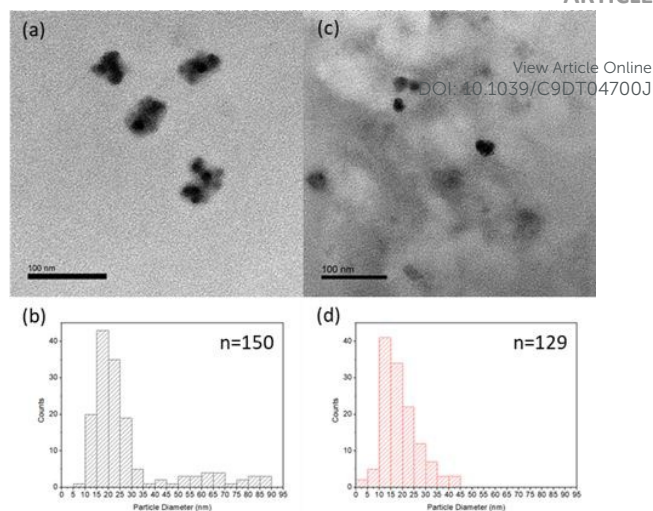

Figure 2: (a) Representative TEM image for compound **1**, additional images available in supporting information. (b) Particle size distribution for compound **1**, where n = 150. (c) Representative TEM image for compound **1-Cl**, additional images available in the supporting information. The dark background is attributed to clumping of BSA. (d) Particle size distribution for compound **1-Cl**, where n = 129.

Results and discussion

Parent compound

During the second and subsequent thermal cycles, [Fe(atrz)$_3$]Cl$_2$ (compound **1**) exhibits a reversible SCO with $T_{1/2}\uparrow$ = 334 K, $T_{1/2}\downarrow$ = 328 K, showing a narrow hysteresis of 6 K, as shown in Figure 1(a).[§] The abruptness of the transition was defined by a 'smoothness' value of 39 K. During the first heating cycle the transition occurs at 361 K, leading to a significant apparent hysteresis for this first cycle only, which is not observed on subsequent thermal cycling. It is common for the first heating cycle to be different from subsequent cycles in many SCO species, particularly the triazole family of complexes,[36,37] and this apparent hysteresis of 33 K has previously been reported for **1**.[38] We attribute this behaviour here to the loss of water during the first heating cycle, as confirmed by thermogravimetric analysis presented in the supporting information (Figure S9 and Table S2). PXRD data for compound **1** are shown in Figure 1(f).

Effect of SSM procedure on SCO properties

SSM requires the further grinding of compound **1**, in the presence of sodium halide salts. A control experiment in which compound **1** was ground in the presence of NaCl for 15 minutes, yielding compound **1-Cl**, was performed in order to distinguish between the effects on the SCO properties of anion exchange and the grinding process. After grinding **1** with NaCl, no chemical differences should be observed and thus the effect of the additional grinding procedure can be evaluated without the possibility of anion exchange taking place.

The PXRD pattern of **1-Cl** is virtually identical to **1**, as shown in Figure 1(f), confirming that the structure is retained after mechanochemical SSM. Coherent crystalline domain size was estimated from peak broadening using the Scherrer equation, revealing a reduction in particle size from 62 nm in **1** to 40 nm in **1-Cl**. The temperature of the SCO reduces slightly from $T_{1/2}\uparrow$ = 334 K, $T_{1/2}\downarrow$ = 328 K in **1** to $T_{1/2}\uparrow$ = 318 K, $T_{1/2}\downarrow$ = 316 K in **1-Cl**, as shown in Figure 1(a). This is accompanied by an increase in 'smoothness', i.e. a more gradual SCO is observed after the SSM procedure (**1** = 39 K compared to **1-Cl** = 55 K). This is consistent with effects of both post-synthetic grinding and particle size reduction previously reported.[32] The differences in the absolute values of $\chi_M T$ are also attributed to these effects.

Due to the high potential error in particle size determination *via* Scherrer analysis,[39] TEM was used to further explore particle size and morphology, as shown in Figure 2.[§§] An average particle size of 28 ± 19 nm was calculated for **1**, based on statistical analysis, with a wide distribution (10 nm to 89 nm). Both the average size (19 ± 8 nm) and the distribution (5 nm to 42 nm) was reduced in **1-Cl**. Further detailed analysis into the effects of mechanochemistry on SCO properties is currently ongoing, but beyond the scope of the present study. However, we can conclude that the effect of the SSM procedure on **1** is to produce a reduction in SCO temperatures of ≈ 12 − 16 K, a reduction in hysteresis width of 3 K and a slight reduction in particle size.

Anion Exchange

Solid state metathesis of compound **1** was carried out using an excess of NaBr, yielding product **1-Br**. The magnetic properties (Figure 1(b)), show a shift of the SCO to significantly lower temperatures ($T_{1/2}\uparrow$ = 298 K and $T_{1/2}\downarrow$ = 295 K) than the control sample, indicating the exchange of chloride for bromide anions in the sample to form [Fe(atrz)$_3$]Br$_2$. The width of hysteresis slightly increased from 2 K to 3 K and abruptness of the SCO remained similar with a calculated 'smoothness' of 41 K

compared to 39 K prior to additional grinding. $[Fe(atrz)_3]Br_2$ has been previously reported to show a significant dependence of its SCO properties on particle size with a range of temperatures reported with $T_{1/2}\uparrow$ = 320 K and $T_{1/2}\downarrow$ = 305 K for macroscopic particles reducing to $T_{1/2}\uparrow$ = 312 K and $T_{1/2}\downarrow$ = 310 K for small (50 nm) particles.[40]

The observed hysteresis for **1-Br** (3 K) is within previously reported values;[40] a complete comparison between experimental and literature values for all complexes is presented in Table 1. The PXRD pattern of **1-Br** reveals differences in the structure of the product when compared with **1-Cl**, as shown in Figure 1(f). The PXRD pattern is similar to previously reported patterns for the complex $[Fe(atrz)_3]Br_2$,[40] with broadening of the peaks attributed to the reduction in the crystallinity, crystalline domain size and the increase in crystalline defects resulting from the grinding process, *vide supra*.

Repeating the SSM procedure on a fresh sample of compound **1** using NaI yielded compound **1-I** as a white powder. A SCO below room temperature was confirmed by analysis of the magnetic properties as shown in Figure 1(c). **1-I** displays SCO temperatures ($T_{1/2}\uparrow$ = 253 K, $T_{1/2}\downarrow$ = 251 K) that are consistent with those previously reported for $[Fe(atrz)_3]I_2$.[41] In contrast to both the observations of our control experiment (**1-Cl**) and the reported effects of grinding on SCO materials, the product maintained a similarly abrupt SCO to the parent compound **1**, with a calculated 'smoothness' = 39 K. The exchange of chloride for iodide anions results in a decrease in both $T_{1/2}\uparrow$ and $T_{1/2}\downarrow$ of >70 K and an increase in abruptness ('smoothness' 55 K to 39 K) when compared with the control sample **1-Cl**.

Table 1: SCO properties for $Fe(atrz)_3A_2$, where A = Cl, Br and I , comparison between literature values and experimental values for anion exchange products.[38,40,41] *Apparent hysteresis

	$[Fe(atrz)_3]Cl_2$	$[Fe(atrz)_3]Br_2$	$[Fe(atrz)_3]I_2$
Lit. $T_{1/2}\uparrow$ (K)	355	312-320	270-280
Lit. $T_{1/2}\downarrow$ (K)	300	304-313	260-278
Lit. ΔT (K)	55*	2-15	8-20

	1	**1-Cl**	**1-F**	**1-Br**	**1-I**
Exp. $T_{1/2}\uparrow$ (K)	334	318	318	298	253
Exp. $T_{1/2}\downarrow$ (K)	325	316	316	295	251
Exp. ΔT (K)	6	2	2	3	2

As seen in Figure 1(f), the PXRD pattern of **1-I** reveals significant differences from **1-Cl**, indicating that anion exchange is accompanied by substantial structural rearrangement.

Literature PXRD data for $[Fe(atrz)_3]I_2$ is not available, therefore comparison with previously reported data was not possible.

Driving Force of Anion Exchange

SSM was shown to successfully exchange the Cl^- anions in compound **1**, for both Br^- (compound **1-Br**) and I^- (compound **1-I**). In literature, ΔH_{rxn}° has been used as a tool to predict the exchange potential for a SSM reaction. Due to the complexity of the iron-triazole chains, calculating enthalpy of formation (H_f°) for compound **1** and the proposed exchange products is beyond the scope of this research. Without enthalpy of formation for the iron-triazole chains, it is not possible to calculate ΔH_{rxn}° and an alternative metric for prediction was required. The total lattice potential energy (U_{POT}) of the sodium halide salts was identified as a suitable alternative due to the availability of values for multiple sodium salts, see Table 2. Assuming the difference in U_{POT} between NaCl and NaX (where X = F^-, Br^-, and I^-), ΔU_{POT}, represents the greatest change in energy occurring during SSM, the complex calculations for the enthalpy of the iron-triazole species complexes can be simplified and U_{POT} can be used as a half reaction addressing the formation of NaCl from NaX. As such, using ΔU_{POT} it is predicted that the chloride anions in compound **1** will exchange with both NaBr and NaI (NaBr - ΔU_{POT} = +37 kJ mol^{-1} and NaI - ΔU_{POT} = +87 kJ mol^{-1}) whereas the exchange with NaF will not proceed (NaF - ΔU_{POT} = -141 kJ mol^{-1}). To test this hypothesis, exchange with NaF was attempted.

Compound **1** was ground with NaF for 15 minutes; yielding **1-F**. It can be seen from the magnetic properties in Figure 1(d) that the sample undergoes SCO that is indistinguishable from the control sample, **1-Cl** ($T_{1/2}\uparrow$ = 318 K, $T_{1/2}\downarrow$ = 316 K and with a 'smoothness' = 55 K). Literature magnetic properties for the compound $[Fe(atrz)_3]F_2$ are not available, and previous attempts to synthesise the complex were unsuccessful, which was attributed at the time to fundamental differences in the radii of the complex cation and anion.[38] The PXRD data of **1-F** is also virtually identical to that of **1-Cl**, and thus it was concluded that it is not possible to access $[Fe(atrz)_3]F_2$ through SSM from compound **1** and NaF, as predicted based on U_{POT} calculations. In order to easily visualise the changing SCO temperatures between different samples, $X_M T$ was normalised within the range 150 – 400 K for all samples, see Figure 1(e).

Table 2: Total lattice potential energies, U_{POT}, for sodium halides (F, Cl, Br and I).[42]

	NaF	NaCl	NaBr	NaI
U_{POT}° (kJ mol^{-1})	910	769	732	682

Extent of Exchange

Iron triazole SCO complexes with mixed ligand systems are known and have been used to tune the switching properties. By contrast, mixed-anion complexes have rarely, if ever, been seen. Hence, having established that it is possible to post-
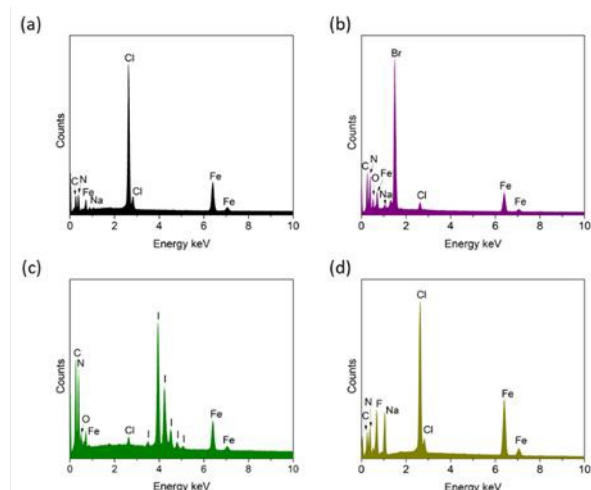
Figure 3: Representative EDX spectra for exchange products, with characteristic energies identified. (a) **1-Cl**, (b) **1-Br**, (c) **1-I** and (d) **1-F**.

synthetically exchange anions in compound **1**, it is important to determine the extent of that exchange.

Energy-dispersive X-ray spectroscopy (EDX) was used to determine the proportion of the various anions present in each sample. EDX spectra for **1-Cl**, **1-Br**, **1-I** and **1-F** are shown in Figure 3. They were used to calculate the relative elemental abundance based upon the characteristic elemental Kα emissions, as summarised in Table S1. For the control sample **1-Cl** the only halide observed was chloride at 16.70 ± 4.85 % by weight. After exchange with NaBr, **1-Br** showed trace chlorine (1.22 ± 0.29 %) and a significant presence of bromine (27.52 ± 4.74 %). In both instances trace sodium (0.36 ± 0.10 % and 0.50 ± 0.10 % respectively) was observed, indicating that unreacted sodium salt was not present in significant quantities. Further, the exchange with NaI, **1-I** showed trace chlorine (0.59 ± 0.05 %) and a significant abundance of iodine (30.21 ± 4.10 %). In **1-I**, no sodium was detected, indicating no unreacted NaI remained in the sample. Thus, it may be concluded that exchange of chloride for bromide or iodide anions proceeds to completion under the SSM conditions employed here.

After attempted exchange of chloride for fluoride, a significant proportion of residual unreacted NaF is present in the washed sample **1-F**. This is attributed to the limited solubility of NaF in methanol and consequently the washing solution used in this study. Additional workup of **1-F** was not carried out in an effort to maintain consistency of the procedure and minimise the potential for solvent effects. This resulted in an overall lower abundance of C, N, Fe and Cl within the sample, as shown in Table S1. The presence of significant quantities of residual NaF is also the likely cause of the low value of $\chi_M T$ for **1-F** at high temperatures observed in Figure 1(d).

Conclusions

Chloride anions in $[Fe(atrz)_3]Cl_2$ can be fully exchanged for bromide or iodide ions by grinding the dry powder in the presence of an excess of the appropriate sodium salt. The exchanged complexes have the SCO properties expected for $[Fe(atrz)_3]Br_2$ and $[Fe(atrz)_3]I_2$. The effect of the additional grinding procedure itself is to slightly decrease $T_{1/2}\uparrow$, $T_{1/2}\downarrow$ and ΔT, in addition to a reduction in abruptness of transition. The propensity for exchange was rationalised using the change in total lattice potential energy of the sodium salts (ΔU_{POT}). Based on the half equation for the formation of NaCl from compound **1** and NaX (where X = F, Br and I), the exchange with both NaBr and NaI was predicted and observed to be successful. However, the exchange using NaF was not predicted to succeed and indeed did not occur. This indicates the formation of stable by-products, in this case NaCl, as the main driving force for this SSM procedure.

The potential to post-synthetically modify the anions of iron triazole complexes provides an additional tool in the discovery of SCO materials. We anticipate that this SSM procedure can be applied to a wide variety of different iron triazole complexes with many different anions in addition to the halides. It is a facile method that will allow access to a wide variety of anions that are typically underexplored in these materials due to limitations of synthetic complexity, commercial availability or differences reagent solubility. We have also demonstrated a simple method for predicting the propensity for exchange to occur with a given set of anions, providing a rational approach to the application of SSM for SCO materials. Furthermore, as SCO materials move ever nearer application, SSM offers a simple post-processing step that could be applied on large scales to access relatively exotic SCO materials from simple and affordable parent complexes.

Conflicts of interest

There are no conflicts to declare.

Acknowledgements

Notes and references

§ Throughout this discussion we report transition temperatures and other characteristics of the SCO measured on the second full thermal cycle. Three full heating and cooling cycles for each compound are shown in the supporting information (Figures S1-5).

§§ In both compound **1** and **1-Cl**, the observed particles were spherical and prone to forming aggregates. To reduce the formation of aggregates, bovine serum albumin (BSA) was added (as described in the experimental section of the supporting

Dalton Transactions Accepted Manuscript

information), the presence of which is visible in the background of Figure 3(c)

1   W. Nicolazzi and A. Bousseksou, *Comptes Rendus Chim.*, 2018, **21**, 1060–1074.

2   A. B. Gaspar, G. Molnár, A. Rotaru and H. J. Shepherd, *Comptes Rendus Chim.*, 2018, **21**, 1095–1120.

3   G. Chastanet, M. Lorenc, R. Bertoni and C. Desplanches, *Comptes Rendus Chim.*, 2018, **21**, 1075–1094.

4   G. J. Halder, C. J. Kepert, B. Moubaraki, K. S. Murray and J. D. Cashion, *Science.*, 2002, **298**, 1762–1765.

5   Z.-P. Ni, J.-L. Liu, M. N. Hoque, W. Liu, J.-Y. Li, Y.-C. Chen and M.-L. Tong, *Coord. Chem. Rev.*, 2017, **335**, 28–43.

6   G. Molnár, S. Rat, L. Salmon, W. Nicolazzi and A. Bousseksou, *Adv. Mater.*, 2018, **30**, 1703862.

7   M. D. Manrique-Juárez, S. Rat, L. Salmon, G. Molnár, C. M. Quintero, L. Nicu, H. J. Shepherd and A. Bousseksou, *Coord. Chem. Rev.*, 2016, **308**, 395–408.

8   L. Salmon and L. Catala, *Comptes Rendus Chim.*, 2018, **21**, 1230–1269.

9   V. A. Varnek and L. G. Lavrenova, *J. Struct. Chem.*, 1995, **36**, 120–127.

10   O. Roubeau, *Chem. - A Eur. J.*, 2012, **18**, 15230–15244.

11   C.-F. Wang, G.-Y. Yang, Z.-S. Yao and J. Tao, *Chem. Eur. J.*, 2018, **24**, 3218

12   A. Enríquez-Cabrera, L. Routaboul, L. Salmon and A. Bousseksou, *Dalton Trans.*, 2019, **48**, 16853

13   Y. Garcia, P. J. van Koningsbruggen, E. Codjovi, R. Lapouyade, O. Kahn and L. Rabardel, *J. Mater. Chem.*, 1997, **7**, 857–858.

14   M. M. Dîrtu, A. Rotaru, D. Gillard, J. Linares, E. Codjovi, B. Tinant and Y. Garcia, *Inorg. Chem.*, 2009, **48**, 7838–7852.

15   J. H. Askew and H. J. Shepherd, *Chem. Commun.*, 2018, **54**, 180–183.

16   S. L. James, C. J. Adams, C. Bolm, D. Braga, P. Collier, T. Friščić, F. Grepioni, K. D. M. Harris, G. Hyett, W. Jones, A. Krebs, J. Mack, L. Maini, A. G. Orpen, I. P. Parkin, W. C. Shearouse, J. W. Steed and D. C. Waddell, *Chem. Soc. Rev.*, 2012, **41**, 413–447.

17   D. E. Crawford, C. K. G. Miskimmin, A. B. Albadarin, G. Walker and S. L. James, *Green Chem.*, 2017, **19**, 1507–1518.

18   J. L. Howard, Q. Cao and D. L. Browne, *Chem. Sci.*, 2018, **9**, 3080–3094.

19   T. Friščić, C. Mottillo and H. M. Titi, *Angew. Chemie Int. Ed.*, , DOI:10.1002/anie.201906755.

20   T. Friščić, *Chem. Soc. Rev.*, 2012, **41**, 3493.

21   Y.-H. Huang, W.-S. Lo, Y.-W. Kuo, W.-J. Chen, C.-H. Lin and F.-K. Shieh, *Chem. Commun.*, 2017, **53**, 5818–5821.

22   T. Friščić and W. Jones, *Cryst. Growth Des.*, 2009, **9**, 1621–1637.

23   T. Friščić, E. Meštrović, D. Š. Šamec, B. Kaitner and L. Fábián, *Chem. - A Eur. J.*, 2009, **15**, 12644–12652.

24   J. Stojaković, B. S. Farris and L. R. MacGillivray, *Chem. Commun.*, 2012, **48**, 7958.

25   R. E. Treece, E. G. Gillan and R. B. Kaner, *Comments Inorg. Chem.*, 1995, **16**, 313–337.

26   I. P. Parkin and A. M. Nartowski, *Polyhedron*, 1998, **17**, 2617–2622.

27   P. Parhi and V. Manivannan, *Solid State Sci.*, 2008, **10**, 1012–1019.

28   H.-J. Meyer, *Dalt. Trans.*, 2010, **39**, 5973–5982.

29   L. Rao and E. G. Gillan, *J. Mater. Res.*, 1995, **10**, 353–361.

30   E. W. Müller, H. Spiering and P. Gütlich, *Chem. Phys. Lett.*, 1982, **93**, 567–571.

31   N. Tsuchiya, A. Tsukamoto, T. Ohshita, T. Isobe, M. Senna, N. Yoshioka and H. Inoue, *Solid State Sci.*, 2001, **3**, 705–714.

32   M. S. Haddad, W. D. Federer, M. W. Lynch and D. N. Hendrickson, *Inorg. Chem.*, 1981, **20**, 131–139.

33   J. Laisney, A. Tissot, G. Molnár, L. Rechignat, E. Rivière, F. Brisset, A. Bousseksou and M.-L. Boillot, *Dalt. Trans.*, 2015, **44**, 17302–17311.

34   B. Michen, C. Geers, D. Vanhecke, C. Endes, B. Rothen-Rutishauser, S. Balog and A. Petri-Fink, *Sci. Rep.*, 2015, **5**, 9793.

35   P. Guionneau, M. Marchivie, G. Bravic, J.-F. Létard and D. Chasseau, in *Spin Crossover in Transition Metal Compounds II*, Springer Berlin Heidelberg, Berlin, Heidelberg, 2004, pp. 97–128.

36   O. Roubeau, J. G. Haasnoot, E. Codjovi, F. Varret and J. Reedijk, *Chem. Mater.*, 2002, **14**, 2559–2566.

37   L. Salmon, G. Molnár, S. Cobo, P. Oulié, M. Etienne, T. Mahfoud, P. Demont, A. Eguchi, H. Watanabe, K. Tanaka and A. Bousseksou, *New J. Chem.*, 2009, **33**, 1283–1289.

38   L. G. Lavrenova, O. G. Shakirova, V. N. Ikorskii, V. A. Varnek, L. A. Sheludyakova and S. V. Larionov, *Russ. J. Coord. Chem. Khimiya*, 2003, **29**, 22–27.

39   M. A. R. Miranda and J. M. Sasaki, *Acta Cryst*, 2018, 54–65.

40   T. Forestier, A. Kaiba, S. Pechev, D. Denux, P. Guionneau, C. Etrillard, N. Daro, E. Freysz and J. F. Létard, *Chem. - A Eur. J.*, 2009, **15**, 6122–6130.

41   L. G. Lavrenova, N. G. Yudina, V. N. Ikorskii, V. A. Varnek, I. M. Oglezneva and S. V. Larionov, *Polyhedron*, 1995, **14**, 1333–1337.

42   D. P, *J. Mol. Struct.*, 1992, **268**, 320.

Dalton Transactions Accepted Manuscript
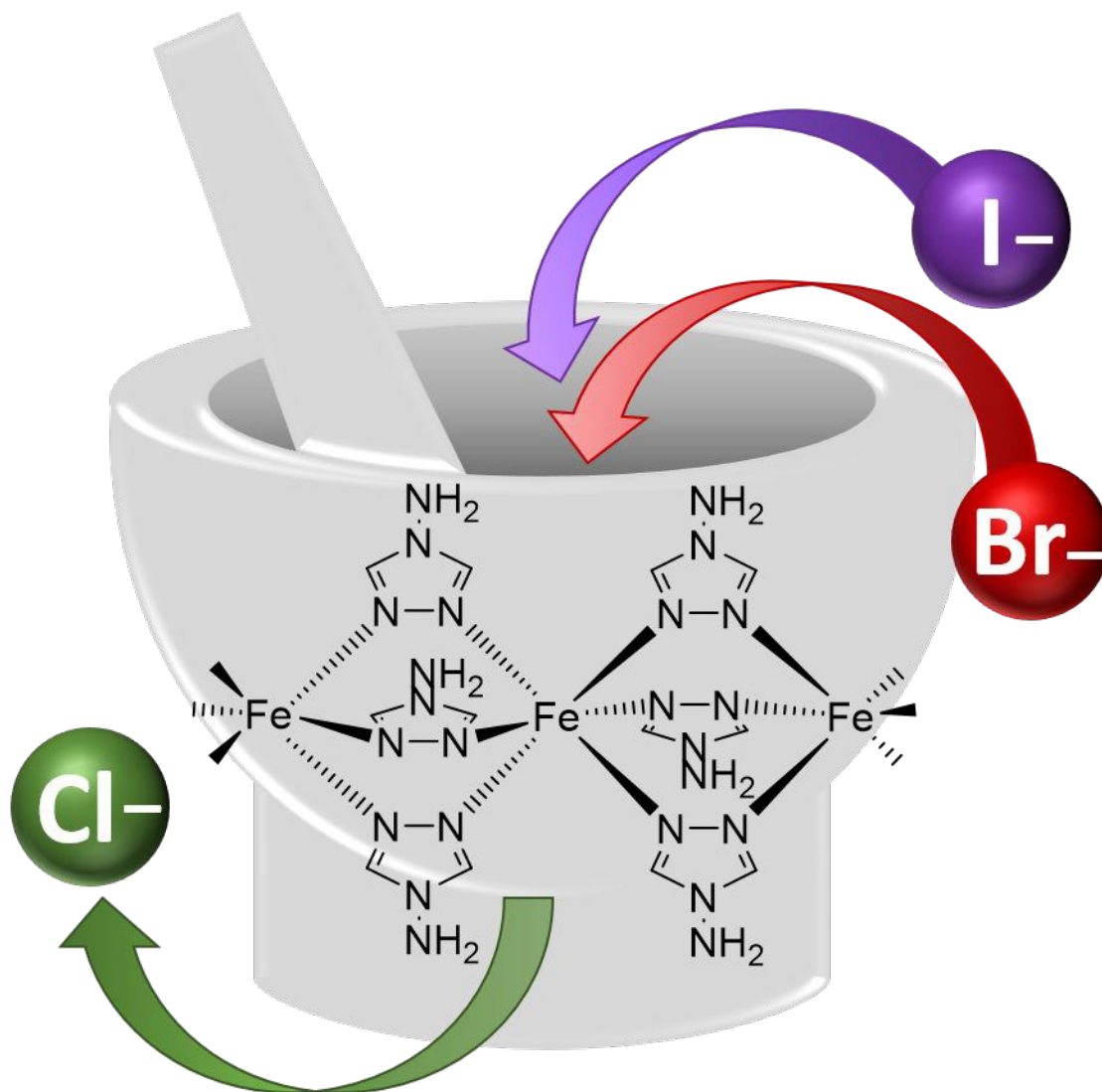
A simple, solvent-free method for post-synthetic exchange of anions in an iron(II) spin crossover material is described.